Large Cyclonic Rings From the Northeast Sargasso Sea

M. S. McCartney, L. V. Worthington, and W. J. Schmitz, Jr.

Woods Hole Oceanographic Institution, Woods Hole, Massachusetts 02543

Expendable bathythermograph observations have revealed large cold core cyclonic current rings to the east of 60°W in a region that mechanical bathythermograph observations (Parker, 1971) indicated to be devoid of rings. As a class these rings are larger than typical Gulf Stream rings that form and drift west of 60°W. The typical diameter (15°C at 500 m) there is around 100 km, while the eastern Sargasso rings are 200 km and more in diameter. Several of these eastern rings were observed on each of four cruises in the northern Sargasso Sea in 1974 and 1975. The overall picture of the region east of 60°W obtained was a very noisy one, dominated by large-diameter, large-amplitude eddies. One of the eastern rings was seen in all four cruises and was observed to drift westward for over 730 km at an average speed of 4.4 km/d, starting at 56°30'W and 34°40'N and passing north of Bermuda. The character of the dissolved oxygen anomalies in the cores of the eastern rings suggests a possible formation region at the eastern end of the Sargasso Sea gyre, around 40°W. Hence the eastern rings may have already been a year old when first observed in November 1974. A single deep hydrographic section showed the center of the deep circulation to lie considerably further southwest than the near-surface circulation center, although this could be a distortion due to a large seamount. Moored current meter data suggest a level of no motion within eastern rings at about 2000 m, giving a weak anticyclonic circulation of 4×10^6 m³/s below that level, compared with the 45×10^6 m³/s cyclonic circulation above 2000 m. On several occasions, smaller-scale upward displacements of the thermal structure were seen at the sides of eastern rings. It is not known whether these represented interactions with smaller rings or some breakdown of the circular symmetry.

Introduction

Cyclonic Gulf Stream rings are formed when a southward meander of the Gulf Stream closes upon itself to the north, cutting off a pool of slope water surrounded by a current ring of warm Gulf Stream water [*Fuglister*, 1972]. This formation process has been observed in some detail [*Fuglister and Worthington*, 1951; *Fuglister*, 1963]. While the surface water mass anomalies quickly disappear, the dynamic current structure and intermediate level water mass anomalies can persist for up to at least 2 years as they drift through the Sargasso Sea [*Cheney and Richardson*, 1976; *Lai and Richardson*, 1977].

The distribution of cyclonic current rings in the Sargasso Sea was examined by *Parker* [1971], using mechanical bathythermograph data from the period 1932–1970. The rings detectable within this shallow data set all fell west of 60°W, with an apparent forbidden region extending east from there to the mid-Atlantic ridge area. Expendable bathythermograph (XBT) observations made in 1974 and 1975 from the area east of 60°W discussed herein demonstrated the existence of large ring structures dominating the hydrographic structure there during this period. *Parker* [1971] gave an average diameter for rings north of 32°N and west of 60°W of 75 km for 17°C at 250-m depth. For comparison, our observations gave a corresponding diameter of 120 km. We will use the name eastern rings for the eastern class of large rings and the usual name of rings for the western class, thus differentiating between the two classes in the discussion that follows.

Lai and Richardson [1977] have taken advantage of the advent of widespread usage of the deeper expendable bathythermograph systems and have reexamined the distribution of rings using XBT data from 1970 to 1976, supplemented by salinity, temperature, and depth hydrographic data. They report several ring sightings in the region east of 60°W, in addition to the eastern ring sightings reported below.

In addition to XBT data, we describe hydrographic data from sections made across eastern rings in November 1974 and again in April 1975, the latter including a deep closely spaced section. Positive oxygen anomalies in the eastern ring cores suggest a formation region at the eastern end of the Sargasso Sea gyre. We had the good fortune to have one eastern ring drift past a mooring instrumented at five levels between 500 and 4000 m. This, together with the deep hydrographic section across the same feature, allows us to examine the horizontal and the vertical structure of the horizontal velocity within this eastern ring.

Data Description

Data sources. The data used in this study came primarily from four cruises, R/V *Knorr* 43, 48, and 49 and R/V *Chain* 118, which span the period from late October 1974 to mid-May 1975, and from a mooring maintained from early August 1974 to May 1975. The first two *Knorr* cruises together were intended to examine the winter renewal of the 18°C water [*Worthington*, 1959] of the Sargasso Sea. A grid of hydrographic stations was occupied, nominally spaced at 1° latitude intervals as shown in Figure 1, with XBTs taken at hourly intervals (15–18 km). A Bermuda–Nova Scotia hydrographic section of deep (to the bottom) stations was made on both cruises to examine seasonal variation in transport. *Knorr* 49 was a mooring setting and pickup cruise. XBTs were taken at hourly intervals along the track shown in Figure 2. This figure also shows the location of the XBT section taken on *Chain* 118 and the location of the mooring. The configuration of the mooring is summarized in Table 1.

XBT data. Eastern rings were first observed on the easternmost pair of sections during *Knorr* 43 (Figure 3). The two bulges along section A-A′ are fairly symmetric, whereas the one along section B-B′ has a rather gentler isotherm slope on its southern side. For the remainder of this paper we will use the 15°C isotherm crossing 500 m to define bulge widths, since the normal depth for the 15°C isotherm in this region is about 600 m. This criterion is, of course, not unique and is only useful for detailed comparison fairly locally. Further west, the normal 15°C depth exceeds 650 m, while to the east it rises to less than 500 m. When this criterion is used, the widths of the three features range from 180 to 230 km. For comparison, the

Paper number 7C0823.
0148-0227/78/027C-0823$03.00

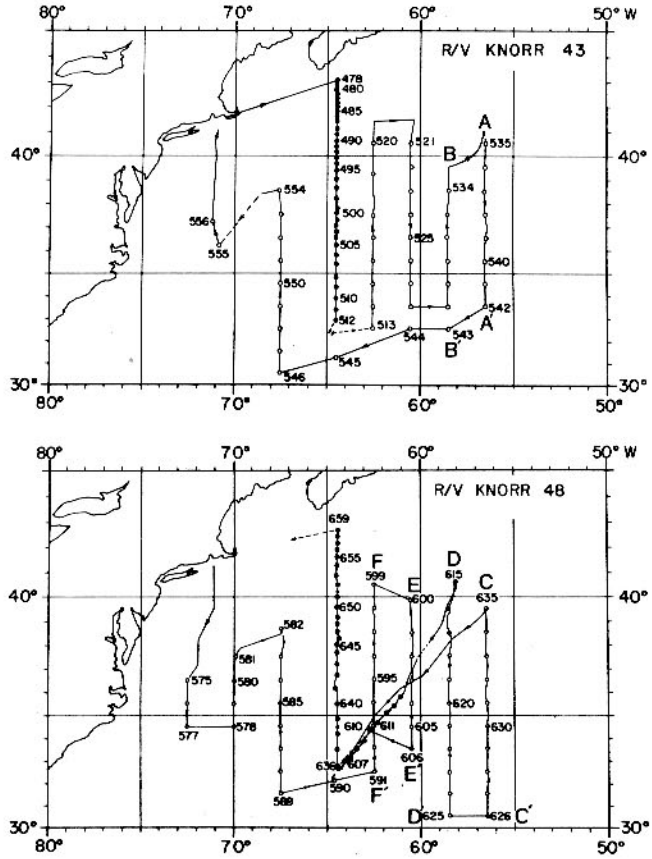

Fig. 1. Cruise tracks and station numbers for R/V *Knorr* 43 (October 26 to November 25, 1974) and 48 (March 7 to April 16, 1975). The open circles are 1000-m hydrographic station locations, the closed circles are deep hydrographic stations to the bottom. XBTs were taken at hourly intervals (15–18 km) along the solid line portions of the tracks but not along the dashed portions. The letter pairs (A-A', etc.) are specific sections shown in Figures 3 and 6.

width of a ring observed during Gulf Stream '60 [*Fuglister*, 1963], which has been referred to by *Barrett* [1971] as '. . . probably the largest ring, both laterally and vertically, which has been studied comprehensively,' was 155 km. The rings described by *Fuglister* [1972] were from 95 to 125 km in diameter. For the long time series of observations of a single ring by *Cheney* and *Richardson* [1976] the ring diameter decreased from 158 to 110 km over a period of 11 months, most of the decay occurring as the ring encountered the Blake Plateau.

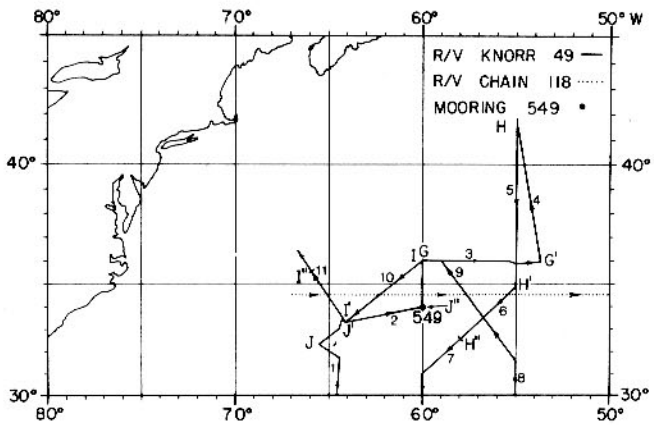

Fig. 2. Cruise tracks for R/V *Knorr* 49 (April 21 to May 19, 1975) and R/V *Chain* 118 (January 22 to February 2, 1975) and the location of Woods Hole mooring 549 (August 9, 1974, to May 1, 1975). The time sequence along the overlapping parts of the *Knorr* track is indicated by the sequential numbering 1–11. Letter groups (J-J'-J") are specific sections shown in Figures 8 and 9.

The eastern rings in Figure 3 do not look as though they were recently formed. There is no indication of a warm ring surrounding the uplifted core, and there is no surface expression of the cold core. The thermocline uplifting within them is quite substantial: the 15°C isotherm rose as shallow as 230 m in the pair on section A-A', while in the one along section B-B' it rose to 330 m. The bulge on the section B-B' had less uplifting and some indication of the 18°C water [*Worthington*, 1959] thermostad over the maximum uplifted region, suggesting that it was crossed off center. The northern bulge along section A-A' contained a 14°C thermostad. This might be a clue to the origin of eastern rings, as will be discussed later, but unfortunately a hydrographic station was not made there.

While no surface signature of the eastern rings was evident in the November data, there was an extensive near-surface signature. Over the bulges the seasonal thermocline gradient below the 100-m surface mixed layer was sharpened by a factor of 2–3. Figure 4 shows this contrast with individual XBT traces. This sharpening occurs not only over the center of each bulge but also well out over the flanks. The width of the increased gradient zone is only slightly less than the 15°C at 500-m width.

Over the next year, several additional encounters with eastern rings occurred. From their observations, summarized in Table 2, we have constructed a chart (Figure 5) showing possible movement paths for what we have inferred to be four distinct eastern rings. Some of the details of their observations are discussed below. Eastern ring A has been crossed several times, in various directions, and our implicit assumption from *Knorr* 43 that we are dealing with more or less circular eddies rather than elongated ridges has been justified. As eastern ring A is the most thoroughly observed, we will discuss it first.

Eastern ring A from *Knorr* 43 was observed successively on *Chain* 118, *Knorr* 48, and *Knorr* 49. The *Chain* 118 sighting (G. Seaver, personal communication, 1975) put it essentially due west of the *Knorr* 43 sighting with an indicated drift speed of 4.2 km/d. Mooring 549 at 60°W, 34°N simultaneously recorded the east to west passage of a cyclonic disturbance, as discussed below. A secondary deformation of the isotherms was found about 200 km further west of the center of the eastern ring on the *Chain* 118 section. It was fairly small in scale, less than 100 km, and apparently interacting with the eastern ring since the 15°C isotherm subsided to only 558 m before rising up to 493 m over the secondary bump. This was the first of several double structures observed, others of which are described below.

TABLE 1. Configuration of Mooring 549 (33°59'N, 60°01'W)

Depth, m	Instrument Type	Start Date	Record Length, days
512	VACM	Aug. 9, 1974	263
812	TP		263
1012	VACM		263
2012	85°T		232
4012	VACM		264

VACM, vector-averaging current meter; TP, temperature-pressure recorder; 850T, 850 burst-sampling current meter with a thermistor.

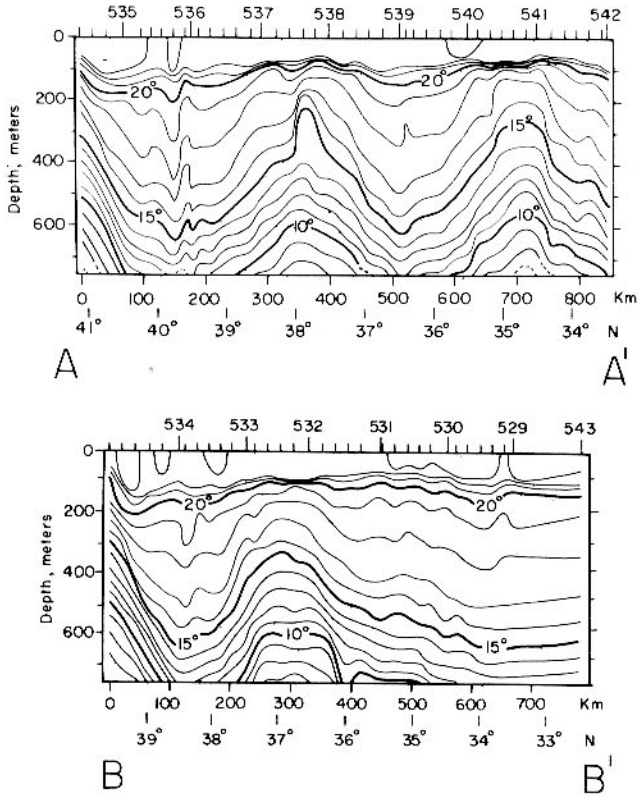

Fig. 3. Temperature sections from R/V *Knorr* 43 XBTs (short tick marks) and hydrographic stations (numbered long tick marks) along 56°30'W (A-A') and 58°30'W (B-B'). Section locations are shown in Figure 1. Data are from November 1974.

During *Knorr* 48, eastern ring A was close to Bermuda. The cruise plan involved two port calls in Bermuda, so in all, four sections were made across eastern ring A, including a line of deep hydrographic stations (607–614, Figure 1), which is separately discussed below.

A particularly noisy image of the Sargasso Sea thermocline topography was obtained on *Knorr* 48. Figure 6 shows the four easternmost meridional sections from this cruise. Eastern ring A appears in section F-F' and is characterized in these late winter–early spring data by a distinctly colder (about 1°C) mixed layer over the center and a sharpened vertical temperature gradient at the base of the mixed layer. This phenomenon is illustrated in more detail by XBT traces in Figure 7. The remaining sections in Figure 6 show a variety of features: meanders, rings, grazing encounters with eastern rings, and depressed thermocline 'dents.' Some of them are discussed below in connection with the other three eastern rings.

Eastern ring A was still near Bermuda during *Knorr* 49, and two separate XBT sections across it were obtained, I-I'-I" and J-J'-J" in Figure 8. A secondary bump was found about 180 km northwest of the eastern ring center. The 15°C isotherm subsides to 520 m in between, then rises to 360 m over the secondary bump. We previously mentioned the *Chain* 118 data showing a similar distortion 200 km west of center 3 months earlier, so it is possible that it represents a long-lived perturbation to the eastern ring structure. It is also possible that the distortion represented a collision with an ordinary scale ring. On *Knorr* 48 the 64°30'W section showed a Gulf Stream ring at about 36°N, i.e., 250 km northwest of eastern ring A. The *Knorr* 49 observation could plausibly be a collision between eastern ring A and this ring.

Eastern ring B is the northern eastern ring on section A-A', Figure 3. The later data (Figure 7 and Table 2) suggest that during *Knorr* 48 this eastern ring lay between D-D' and E-E'. In Figure 6 these two sections have uplifted regions where 15°C rises to 470°, both times with distinctly colder water, less than 18.4°C, above the maximum uplifted zone. These observations are interpreted as indicating an eastern ring lying between the two section lines, which are 180 km apart at 36°N. The 40-km differences in latitude of the maximum uplifting would be either an asymmetry in shape or a southward drift component over the 10 days between the two sightings. Another possible grazing encounter with eastern ring B occurred on section I-I'-I" (Figure 8) of *Knorr* 49, where a secondary uplifted region with a cold spot above it can be seen at 61°25'W.

Eastern ring C was first detected on section C-C' of *Knorr* 48 (Figure 6). The section shows a rather young ring at 37°20'N and an eastern ring with a double-humped structure. Over the southern hump the eastern ring cold spot is 17.6°C. Over the northern hump the mixed layer was distinctly warmer, 18.3°C, perhaps indicating the influence of warm Gulf Stream water recirculating around the ring to the north. Perhaps the ring contributed to the peculiar shape of eastern ring C. On *Knorr* 49 a month later, C was again encountered. Sections G-G' and H-H'-H", shown in Figure 9, crossed at right angles to each other approximately at the center of eastern ring C. It no longer exhibited a close double-hump structure. Instead there is a nearly separated bump about 250 km west of the main uplifted region. The latter has a winter mixed layer remnant at 17.5°, suggesting identification of this main uplifted region with the southern hump on section C-C'. The smaller bump probably then corresponds to the northern hump on section C-C': the mixed layer is warmer, and in between the two uplifted regions the 18°C isotherm is between 150 and 200 m, as it was on section C-C'.

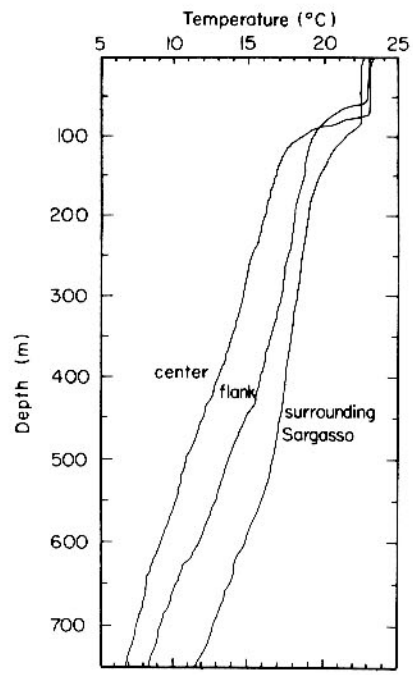

Fig. 4. Selected XBT temperature-depth traces illustrating the sharpening of the seasonal thermocline gradient at 100 m in November over the eastern rings compared with the surrounding Sargasso Sea. The XBTs are 277 (center, 34°39'N, 56°29'W), 280 (flank, 34°06'N, 56°27'W), and 268 (surrounding Sargasso, 36°13'N, 56°31'W) all taken on November 15, 1974, on R/V *Knorr* 43.

TABLE 2. Summary of Big Baby Observations Plotted in Figure 9

Code	Date	Ship	Cruise	15°C Minimum depth, m	15°C at 200-m Width, km	Latitude	Longitude	Drift Speed, km/d
A_{43}	Nov. 15, 1974	*Knorr*	43	270	230	34°40'N	56°30'W	4.2
A_{118}[a]	Jan. 24, 1975	*Chain*	118	230	210	34°30'N	59°40'W	4.6
A_{48}	March 25, 1975	*Knorr*	48	215	260	34°20'N	62°40'W	4.7
A_{49}[b]	April 29, 1975	*Knorr*	49	235	160	33°20'N	64°00'W	
B_{43}[c]	Nov. 15, 1974	*Knorr*	43	230	190	37°50'N	56°30'W	2.7
B_{48a}	March 19, 1975	*Knorr*	48	475	50	36°10'N	60°30'W	
B_{48}[d]	March 24, 1975	*Knorr*	48			35°50'N	59°30'W	
B_{48b}	March 29, 1975	*Knorr*	48	470	50	35°30'N	58°30'W	3.5
B_{49}	May 17, 1975	*Knorr*	49	540		35°10'N	61°25'W	
C_{48}[e]	April 2, 1975	*Knorr*	48	390	130	35°30'N	56°30'W	
C_{49}[f]	May 8, 1975	*Knorr*	49	270	140	35°40'N	55°25'W	4.1
C_{175}[g]	Dec. 8, 1975	*Trident*	175	170	190	34°40'N	65°00'W	
D_{43}[h]	Nov. 12, 1974	*Knorr*	43	330	180	36°55'N	58°30'W	5.0
D[i]	March 24, 1975	AXBT		200	130	36°30'N	65°50'W	

[a]Secondary bump 200 km west of center with 15°C rising to 493 m and falling to only 558 m in between (G. Seaver, personal communication, 1975).
[b]Secondary bump 130 km northwest of center with 15°C rising to 360 m and falling to only 520 m in between.
[c]14°C thermostad in core.
[d]Position and date inferred from the grazing encounters B_{48a} and B_{48b}.
[e]Double-humped structure possibly distorted by interaction with nearby ring.
[f]Secondary bump 230 km west of center with 15°C rising to 480 m and falling to only 580 m in between.
[g]P. Richardson (personal communication, 1975).
[h]Elgonated southern flank.
[i]Starting point of a time series of observations. *Lai and Richardson* [1977] ring D. Uplifting and diameter from P. Richardson (personal communication, 1975) observation on June 7, 1975.

An eastern ring surveyed north of Bermuda on *Trident* 175 (P. L. Richardson, personal communication, 1976) some 8 months after *Knorr* 49 presents a problem. It could be a fifth eastern ring not previously sighted, eastern ring A essentially stationary for 8 months, eastern ring B drifting to the west at less than 2 km/d, or eastern ring C moving at just over 4 km/d. We have grouped it with eastern ring C, since the 4.1-km/d drift speed this implies is similar to what we observed for eastern ring A in the same general region. This is, however, a very arbitrary assignment; more data from this region and period may later clarify the situation.

A last possible association has been indicated in Figure 5 and Table 2 between eastern ring D, observed in section B-B' (Figure 3) and an 18-month sequence of observations reported by *Cheney* and *Richardson* [1976] as 'ring D.' Drifting west at 5 km/d, the timing would be such that the XBT grid of *Knorr* 48 and 49 would have missed it.

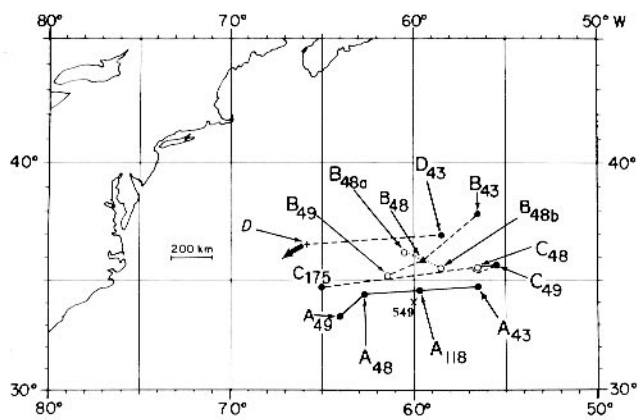

Fig. 5. Summary chart of eastern ring sightings and inferred movements. The solid circles are central crossings, where 15°C rose higher than 400 m. The open circles are grazing encounters where 15°C remained deeper than 400 m. The details of each observation are summarized in Table 2, using the subscripted letters. The unsubscripted D is the first observation in a 17-month time series of drift to the southwest given by *Lai and Richardson* [1977]. The solid line shows the likely drift path of ring A, while the dashed lines show some possible paths for the other observations.

Hydrographic data. In the process of a Gulf Stream meander pinching off to form a Gulf Stream ring, a core of slope water is cut off, which then is carried with the ring as it moves through the Sargasso Sea [*Fuglister*, 1972]. This core retains anomalously low salinity and high dissolved oxygen throughout the lifetime of the ring. If eastern rings also are formed by such a process, then they will show anomalous water characteristics in their interior, presuming that the current involved in the meander separated two distinct water masses. On the other hand, if the eastern rings were locally formed by, say, midocean baroclinic instability, then no such anomalous water would appear. The hydrographic data show the former to be the case.

In Figure 10, temperature-dissolved oxygen and temperature-salinity diagrams are shown for two subsets of the hydrographic data from *Knorr* 43 and 48. The subsets are the stations with 15°C shallower than 400 m, representative of the interior of the eastern rings, and the adjacent stations with 15°C deeper than 500 m, representative of the undisturbed local Sargasso Sea environment. This selection allows clearer distinction between the water masses involved, since it excludes stations falling at the outer flanks of the eastern rings, where mixing has created an intermediate characteristic water mass. For comparison, the solid curve shows the *Richards and*

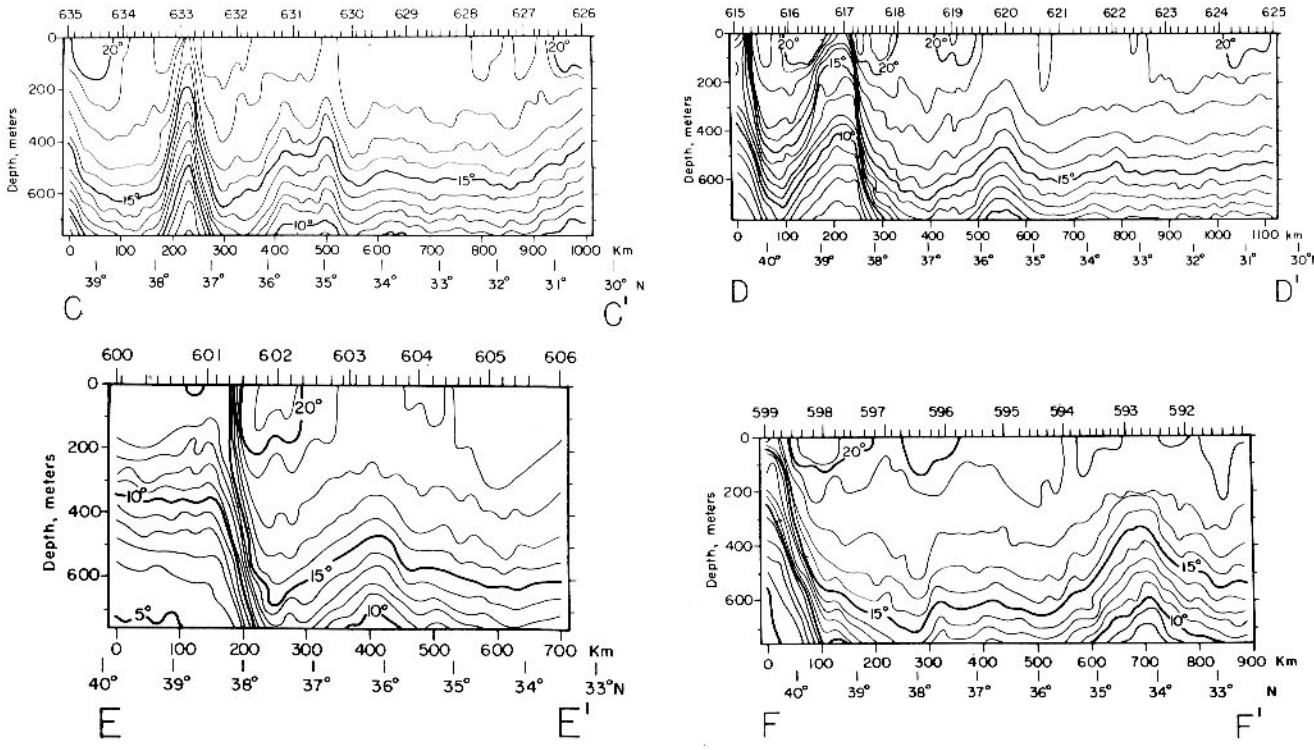

Fig. 6. Temperature sections from R/V *Knorr* 48 XBTs (short tick marks) and hydrographic stations (numbered long tick marks) along 56°30'W (C-C'), 58°30'W (D-D'), 60°30'W (E-E'), and 62°30'W (F-F'). Section locations are shown in Figure 1. Data are from mid-March to early April 1975.

Redfield [1955] density-dissolved oxygen curve converted to temperature-dissolved oxygen by the mean temperature-density relation in the Sargasso Sea and corrected for pre-1959 oxygen processing differences. The *Knorr* 48 mixed layer data are distinctly colder, higher in oxygen, and lower in salinity over the eastern rings than in the surrounding Sargasso. These colder mixed layers were the closest to actual 18°C water [*Worthington*, 1959] renewal that we found in 1975. Both data sets show separation above about 12° or 13°C. The oxygen data symbols for stations 541 and 593 are connected by curves. These two stations are the most centrally located and show the largest, most systematic offsets. The eastern ring data indicate dissolved oxygen values of about 0.4 ml/L higher than the surrounding Sargasso water in the temperature range 13.0°–16.5°C. The salinity data are less distinctly separated, but there is a definite splitting of the data envelopes above 14.5°C.

J. Gould (personal communication, 1976) has suggested that eastern rings might originate at the eastern end of the Sargasso Sea gyre, near 40°W, where generally a fairly abrupt termination of the 18°C water thermostad and a density front occur. He has observed an eastern ring in this region, as has G. Seaver (personal communication, 1975). If this is the formation region, the water mass characteristics within the core of the eastern rings should be related to that characteristic of the area east of this front. Included on the temperature-oxygen diagram of Figure 10 are data from the area to the east of the 18°C water termination along 36°15'W. The eastern ring data in Figure 10 (about 20° west of this supposed formation site) are intermediate in anomaly between the Sargasso data (approximately zero anomaly) and the data east of 40°W at temperatures above 10°C. The salinity data east of 40°W also show slightly lower values above 15°C, but since this is the seasonally influenced upper 200 m, they cannot be used conclusively in comparison to the eastern ring low-salinity values above 14.5°C.

The data east of 40°W also show high oxygen at temperatures below 10°C. This reflects Mediterranean influence, with associated positive salinity anomalies. There is no corresponding high-oxygen, high-salinity anomaly evident in the deep-

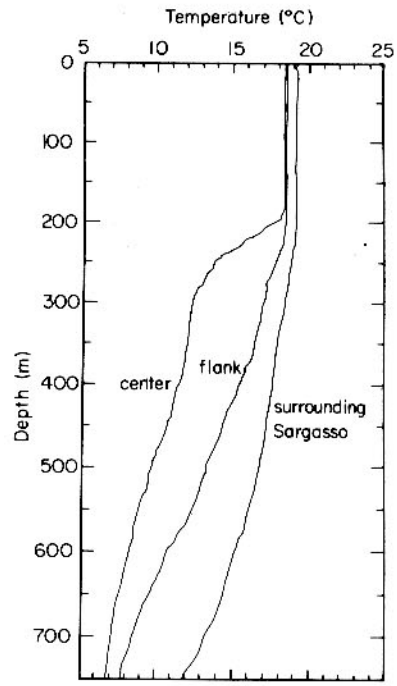

Fig. 7. Selected XBT temperature-depth traces illustrating the colder mixed layer in March over the eastern rings compared with the surrounding Sargasso Sea and the sharp gradient below the mixed layer over the immediate center. The XBTs are 283 (center, 34°07'N, 62°48'W), 285 (flank, 34°32'N, 61°26'W), and 289 (surrounding Sargasso, 35°19'N, 61°37'W), all taken on March 25, 1975, on R/V *Knorr* 48.

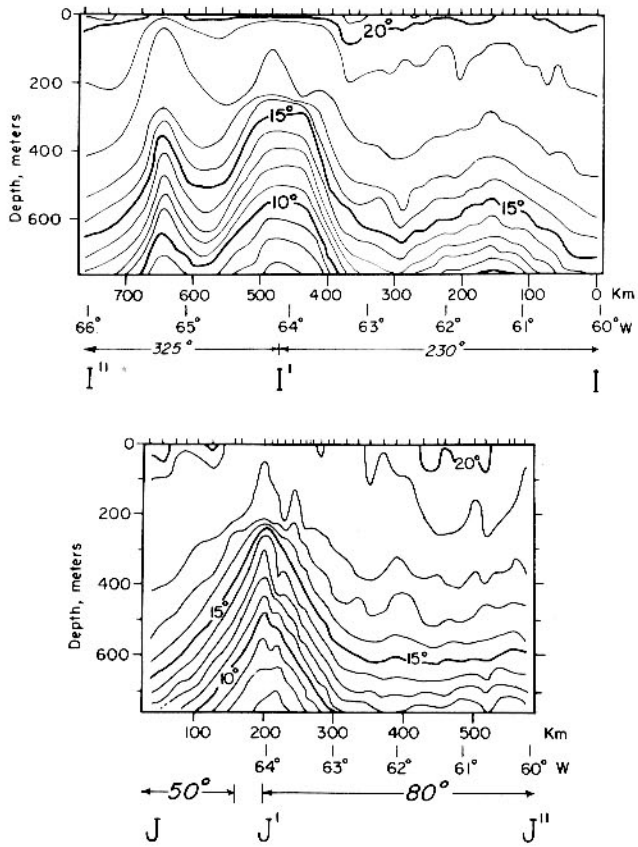

Fig. 8. Temperature sections from R/V *Knorr* 49 XBTs (short tick marks), crossing an eastern ring at 33°20'N, 64°00'W. Section locations are shown in Figure 2. Data are from late April (J-J'-J") and mid-May (I-I'-I").

water of the eastern rings. This is not necessarily an argument against this formation region. Particle trajectories cease to close in a current ring at depths below where the cyclonic circulation speed approximately equals the drift speed, and water there is not carried along with the ring as it drifts. An interpretation of the data in Figure 10 then is that within the eastern rings, only water warmer than about 13°C is being advected with them. This corresponds to a depth over the center of the eastern rings of around 350–400 m and somewhat deeper over the flanks.

The potential temperature field from the deep hydrographic section run on *Knorr* 48 northeast from Bermuda is shown in Figure 11. The cold spot and sharp gradient at the base of the mixed layer are evident. There is a 12°C thermostad in the center of the eastern ring. The 'center' XBT in Figure 7 shows this thermostad. The temperature contours in Figure 11 suggest a tilt of the axis, with the near-surface isotherm having maximum uplifting near station 610, while in the deepwater the maximum uplifting shifts to the southwest, falling at station 609 at 2000 m and at station 608 at 4000 m. It is not known whether this tilt is a property of eastern rings or represents a distortion due to Muir Seamount (rising shallower than 2000 m between stations 609 and 610). The section orientation prevents us from saying whether this axis tilt was north-south, east-west, or a combination. There is one documented case of a ring with a north-south axis tilt. *Fuglister*'s [1972] north-south section through his 'western' ring indicated the center to be 50 km further south in the deepwater. This particular ring had a 15°C at 500-m diameter of 95 km. An east-west section through the same ring (F. C. Fuglister, personal communication, 1976) showed no axis tilt.

In Figure 12 the geostrophic velocity field and transport relative to the bottom are shown. The tilt indicated in the temperature field also shows up in the velocity field. The cyclonic circulation, not including the reversed piece to the northeast between stations 613 and 614, is about 48×10^6 m^3/s. The reversal of the velocity which occurs between stations 613 and 614 is consistent with our inferred position of a second eastern ring at 35°50'N, 59°30'W, 140 km east of station 614. The indicated southeast velocity would be the beginnings of the cyclonic circulation of this eastern ring.

Moored current and temperature data. Temperature and velocity vector time series (Figure 13) from mooring 549 (Table 1) have been low-pass-filtered in order to remove fluctuations with periods of less than 1 day, and temperatures have been linearly corrected for mooring motion. The temperature records are dominated by a cold event (temperature decrease of about 3.5°C at 512 m) in January–February 1975, and these low temperatures are associated with high velocities in the thermocline. Eastern ring A (Figure 5, A_{118}) was observed (*Chain* 118, G. Seaver, personal communication (1975)) to be slightly north and east of mooring 549 at the end of January 1975 and to the west and slightly north on *Knorr* 48 (A_{48}, Figure 5). Thus the ring passage indicated in the mooring time series is supported by XBT sections during and after its observation at the mooring.

At 512 m in Figure 13 the coldest temperature is 13.0°C, indicating by reference to Figure 11 that the center of the eastern ring A passed north of the mooring by about 50 km. That the center passed north rather than south of the mooring

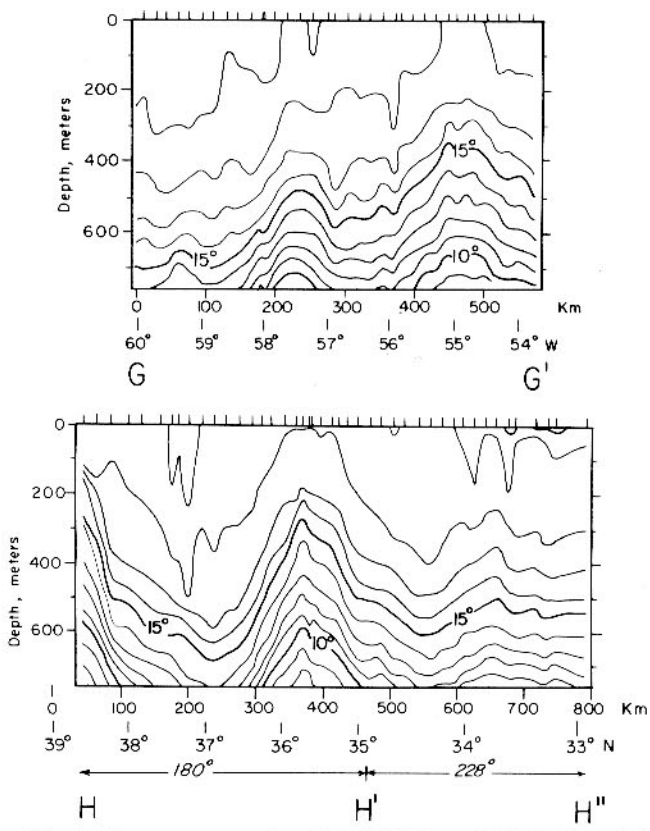

Fig. 9. Temperature sections from R/V *Knorr* 49 XBTs (short tick marks), crossing an eastern ring at 35°40'N, 55°25'W. Section locations are shown in Figure 2. Data are from May 1975.

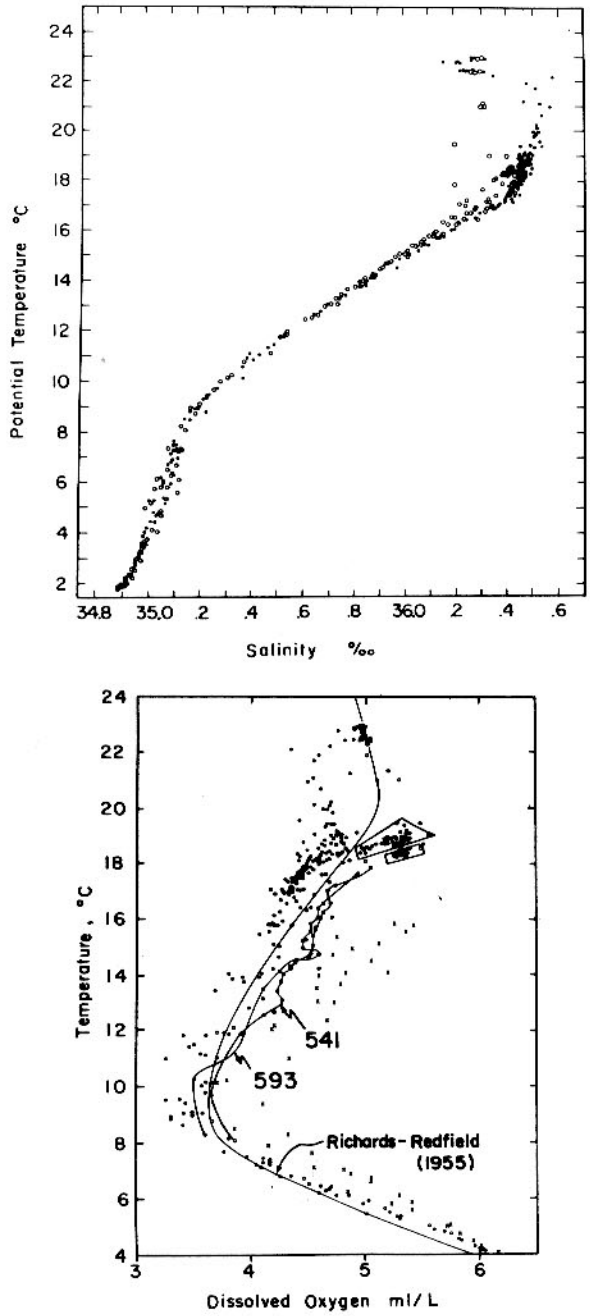

Fig. 10. Temperature-dissolved oxygen and potential temperature-salinity diagrams for *Knorr* 43 and 48 hydrographic data in and near eastern rings. Open circles are data from stations with 15°C shallower than 400 m and characterize the interior of eastern rings. The solid circles are from adjacent stations where 15°C is deeper than 500 m. The temperature-oxygen data for temperatures between 8° and 18°C are connected for stations 541 and 593. The two boxes enclose the *Knorr* 48 mixed layer data. The crosses are data from R/V *Atlantis II* 9 (stations 321, 322, and 323, February 1964) east of 41°W along 36°15'N with temperatures colder than 16°C. Potential temperature was used with the salinity data to show that the small separation of the two sets of data was not simply due to the different pressure levels that a given salinity is found inside the eastern rings in comparison with outside.

is suggested by the likely path of A in Figure 5 and is confirmed by the velocity vector time series. The velocity vectors at 512 and 1012 m rapidly increase in magnitude and point southeast in early January 1975, then rotate counterclockwise to east around the beginning of February, when the associated temperatures are coldest. It swings counterclockwise further, abruptly decreasing in magnitude while pointing to the northeast at the end of February. This sequence is consistent with a cyclonic ring passing from east to west to the north of the mooring. Maximum speeds at 512 m are about 45 cm/s, which is, as would be expected, somewhat higher than the highest 500-m geostrophic velocities computed from the deep hydrographic section relative to the bottom (Figure 12).

The XBT section yielding sighting A_{118} (G. Seaver, personal communication, 1975) also showed a secondary deformation or hump 200 km west of the center of A_{118}, separated from A by a small warm spot. Preceding the eastern ring event a

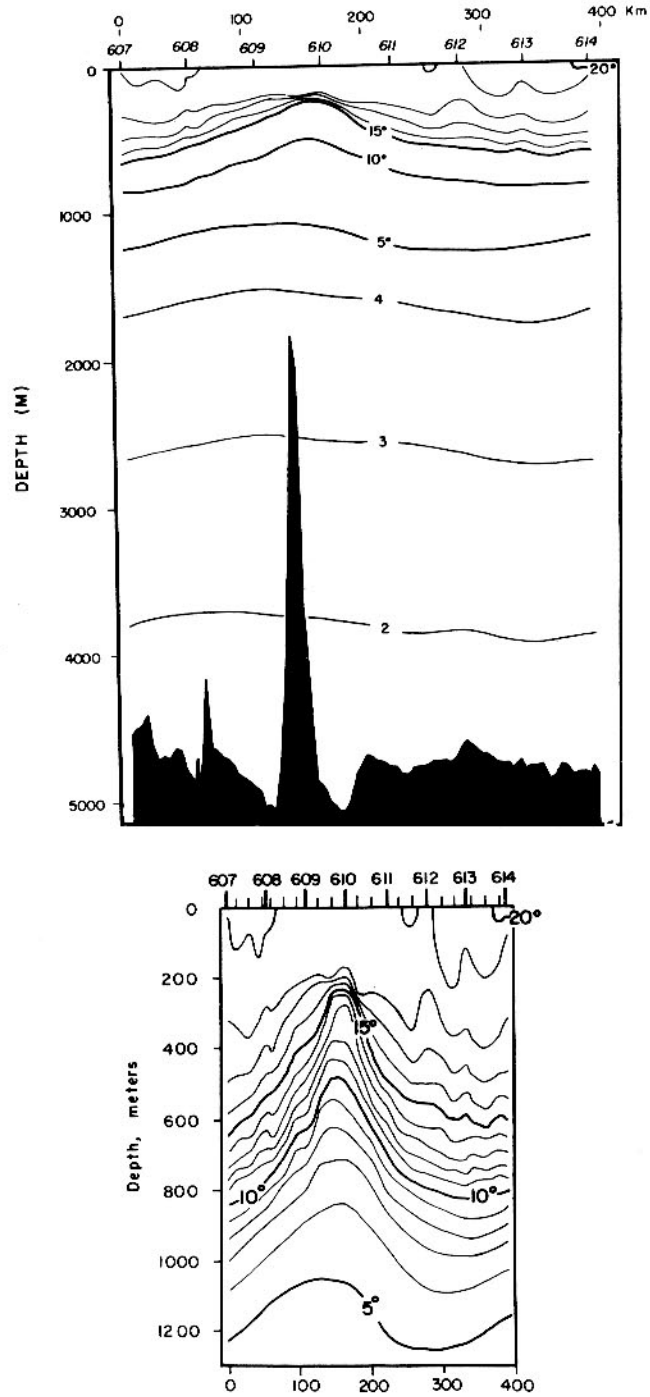

Fig. 11. Potential temperature section from the deep hydrographic section (Figure 1) across eastern ring A (A_{48} in Figure 5 and Table 2). The section has been detailed above 760 m by XBT data.

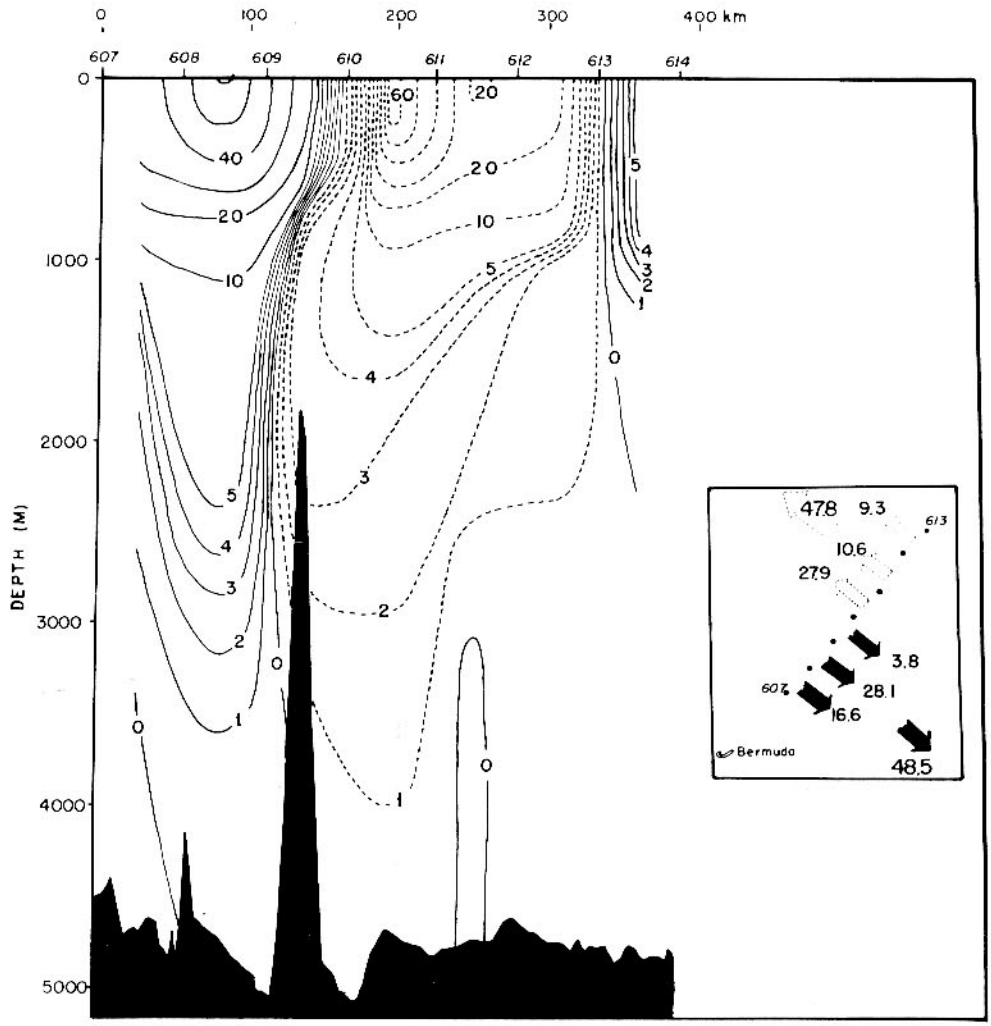

Fig. 12. Geostrophic velocity (in centimeters per second) section and volume transports (in 10^6 m^3/s) relative to bottom for the deep hydrographic section (Figure 1) across eastern ring A (A_{48} in Figure 5 and Table 2).

smaller-amplitude and shorter-duration cold-warm oscillation was observed at around the third week in December at 812 and 1012 m (Figure 13), with a less evident signal at other depths. At a westward drift speed of 4.6 km/d (Table 2) the cold event would precede the eastern ring A by 43 days, giving the observed (Figure 13) cold event at the mooring in the third week of December. The temperature structure of the upper 750 m of the bump did show a larger signal at 750 m than at 500 m, consistent with the mooring data. The width of the bump was about 100 km, or a duration of about 3 weeks at 4.6 km/d. For the 2 weeks preceding the third week of December the velocity vectors at 512 and 1012 m were basically southeast. They rotated clockwise and decreased in magnitude, being near zero in the third week of December and then increasing in magnitude while pointing northwest the next 2 weeks.

Although velocities at 512 and 1012 m in Figure 13 are clearly consistent with a cyclonic ring passage, the 2012- and 4012-m data are more difficult to interpret. As an aid in description, the means have been subtracted from the records at each depth, for the velocity components as well as horizontal vector time series (Figure 14). Two estimates of the mean were used (Table 3): the time average of the full record and a 'special mean' defined as the average with the data during the influence of the ring passage deleted (December 15, 1975, to March 15, 1976). It is difficult to associate the 2012- and 4012-m velocities with a cyclonic disturbance.

During the passage of A over 549 the velocities at 2012 and 4012 m were comparatively small. The effect of the passage of the eastern ring is to reduce substantially the 4012-m velocities, whereas the signal at 2012 m is comparatively low throughout the record. In Figure 15 the geostrophic velocities and transports for the deep hydrographic section on *Knorr* 48 (Figure 11) are recalculated in relation to a reference level of 2000 m. There is, of course, now an anticyclonic disturbance below 2000 m, transporting about 4×10^6 m^3/s with maximum calculated velocities of about 5 cm/s. *Schmitz* [1977] finds that the deep zonal velocities under the mean position of the near-surface Gulf Stream axis are, on the average, in the westward direction. The deep anticyclonic circulation beneath the main eastern ring cyclonic circulation might arise from the pinching off of a meander of this superimposed strong eastward, weak westward current. Is the 4012-m record consistent with the passage of an anticyclonic disturbance? The temperature field is unaffected by the reference level, so only the velocity records can be used to check. The 4012-m disturbance velocity stays in the northeast quadrant in December, January, and most of February, with a slow decrease in magnitude during the latter part of February, switching to southwest at the beginning of

March. This nearly unidirectional disturbance does not seem to be consistent with the passage of an anticyclonic disturbance.

It does not appear possible then to describe the eastern ring signal in the 4012-m data simply as the passage of either a cyclonic or anticyclonic disturbance. The field in Figure 15 contains the eastern ring disturbance field and the mean flow. Since the 4000-m anticyclone in Figure 15 is asymmetric, an attempt was made to see if subtracting the component of mean flow normal to the hydrographic section would lead to a jetlike asymmetric flow. This approach also fails; the effect of this subtraction makes the anticyclonic flow at 4000 m in Figure 15 more symmetric.

Discussion and Summary

Perhaps the most significant aspect of the observations we report on here is the extraordinarily noisy snapshots of the hydrography of the region northeast of Bermuda that we obtained (Figures 3, 6, 8, and 9). This may not be the ordinary state of affairs: the geostrophic transports measured on the *Knorr* 43 and 48 64°30'W deep hydrographic sections were the lowest ever recorded, which may indicate an unusual situation. On the other hand, both the Gulf Stream '60 [*Fuglister*, 1963] and the IGY sections [*Fuglister*, 1960] showed large-scale bumps in the same area, although not as dramatic as, say, section A-A' in Figure 3. *Dantzler* [1977] has produced a chart of estimates (from XBT data) of the eddy potential energy for two-degree squares over the North Atlantic. The maximum values, of course, are found at the mean Gulf Stream path. High values are found only west of 40°W, in an oval area agreeing quite well with the Sargasso gyre of *Worthington*'s [1976] two-gyre North Atlantic gyre, and east of 60°W, at the same latitudes where we observed eastern rings. A new picture is emerging of the North Atlantic, of a northwestward concen-

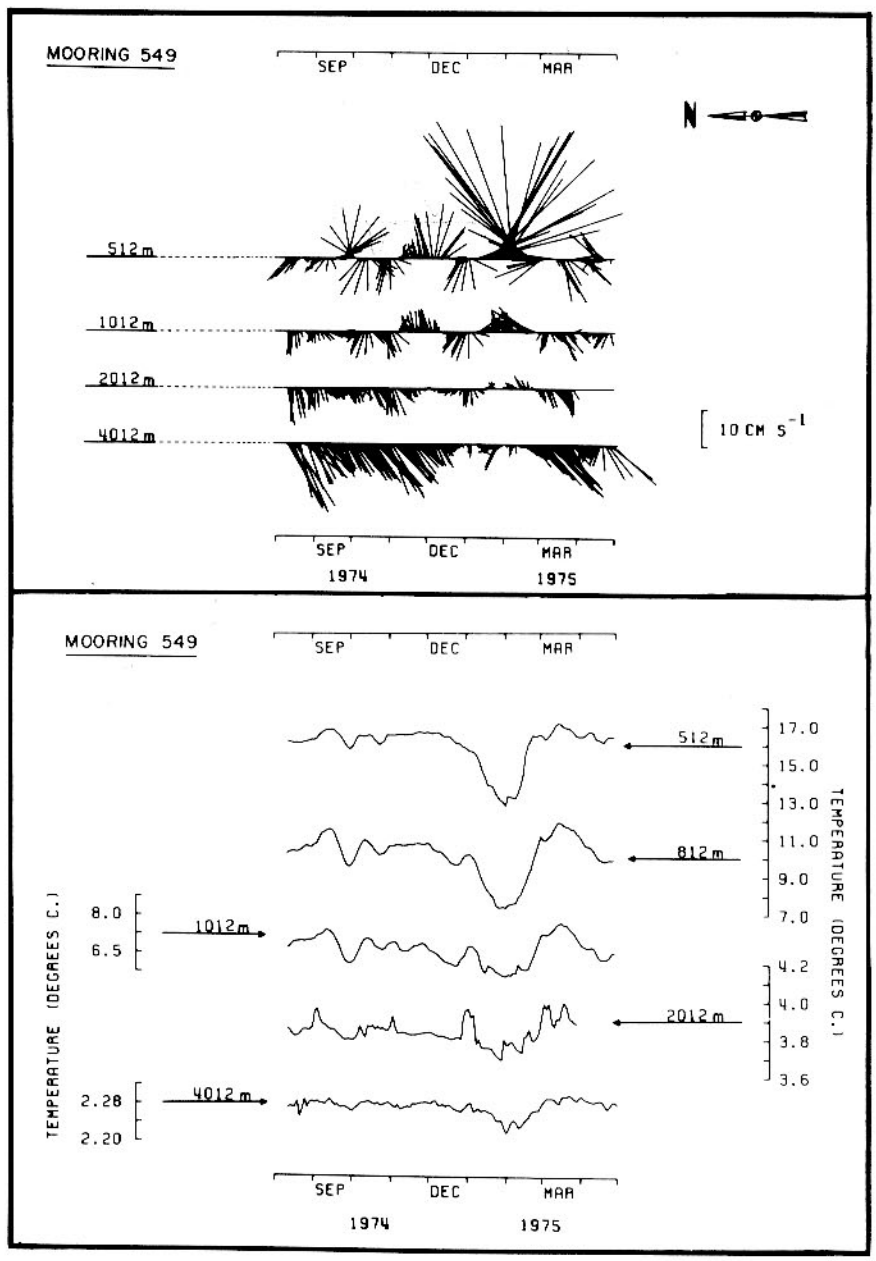

Fig. 13. Temperature and velocity vector time series from mooring 549 (Table 1).

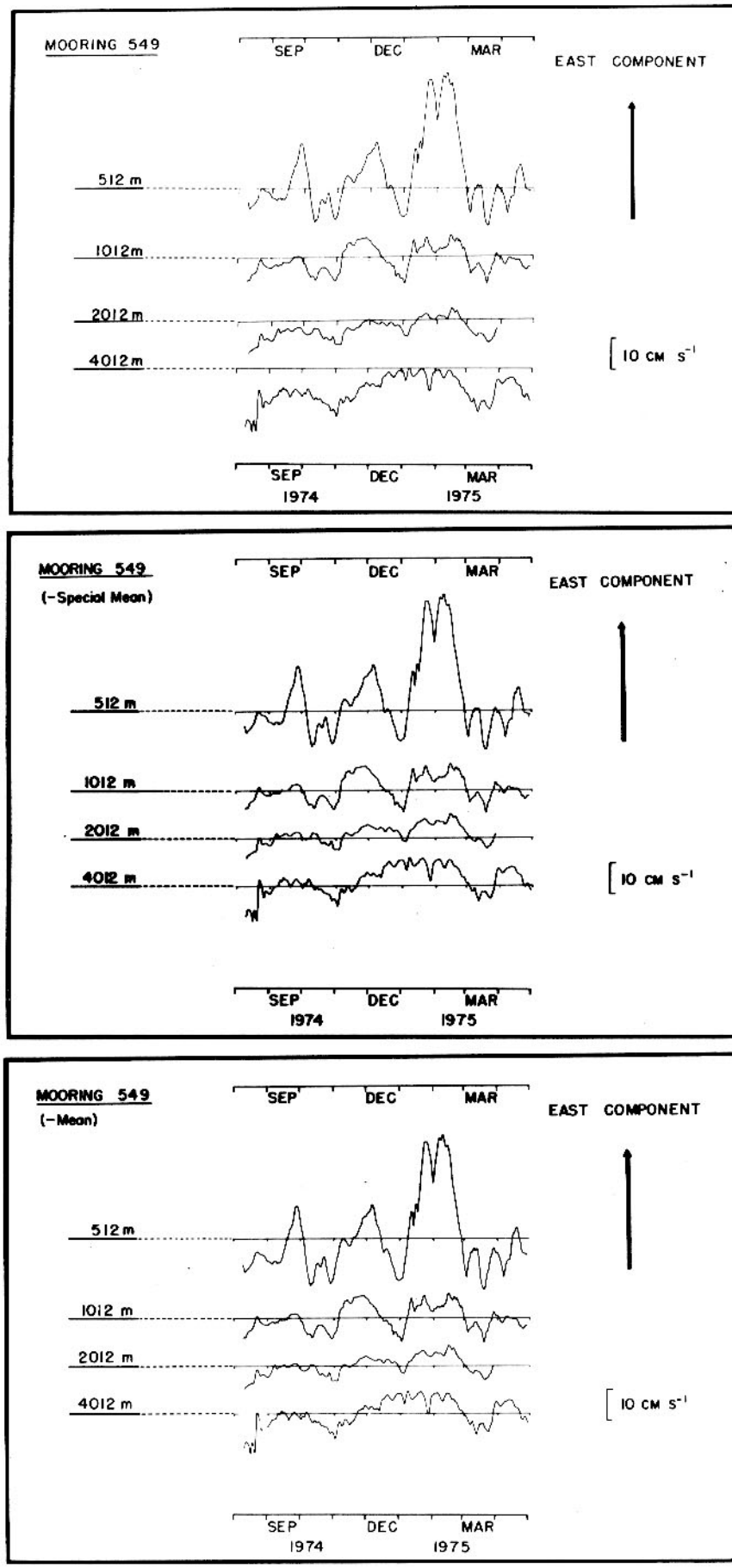

Fig. 14*a*

Fig. 14. Velocity component and velocity vector time series from mooring 549 (Table 1). The means subtracted to give the disturbance velocities are tabulated in Table 3.

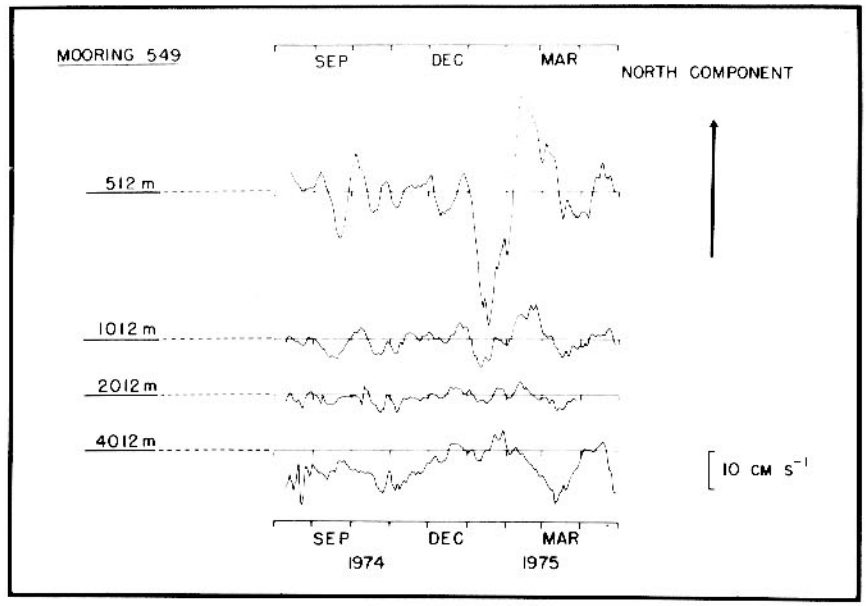
MOORING 549
SEP
DEC
MAR
NORTH COMPONENT
512 m
1012 m
2012 m
4012 m
10 CM S⁻¹
SEP
DEC
MAR
1974
1975

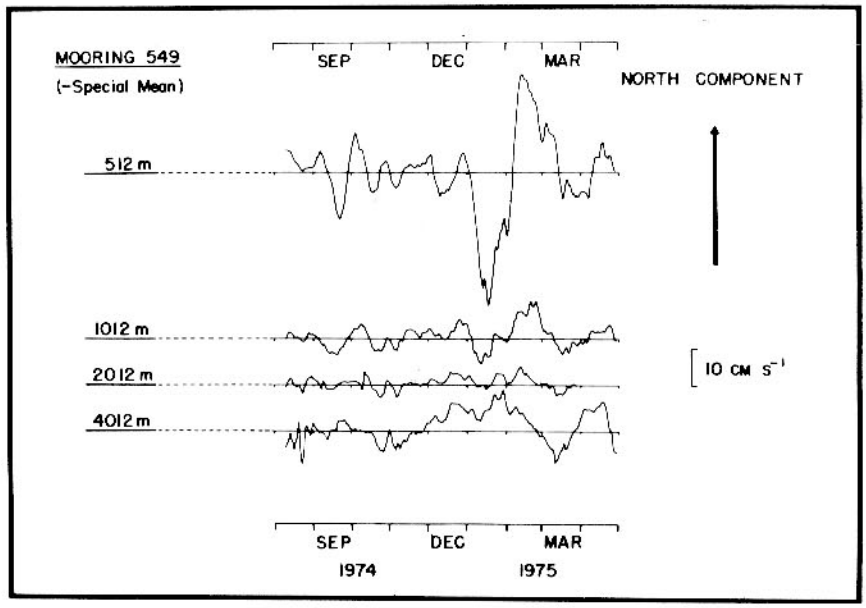
MOORING 549
(-Special Mean)
SEP
DEC
MAR
NORTH COMPONENT
512 m
1012 m
2012 m
4012 m
10 CM S⁻¹
SEP
DEC
MAR
1974
1975

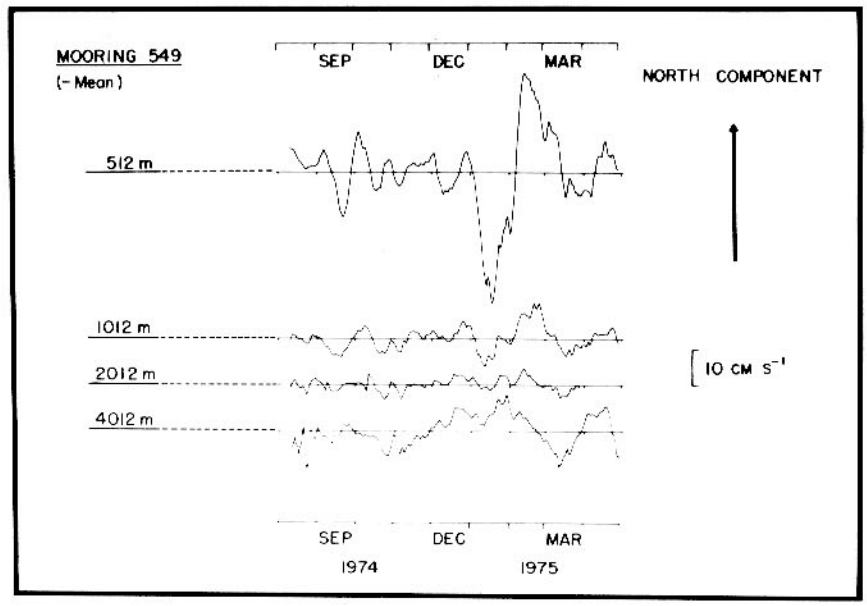
MOORING 549
(- Mean)
SEP
DEC
MAR
NORTH COMPONENT
512 m
1012 m
2012 m
4012 m
10 CM S⁻¹
SEP
DEC
MAR
1974
1975

Fig. 14*b*

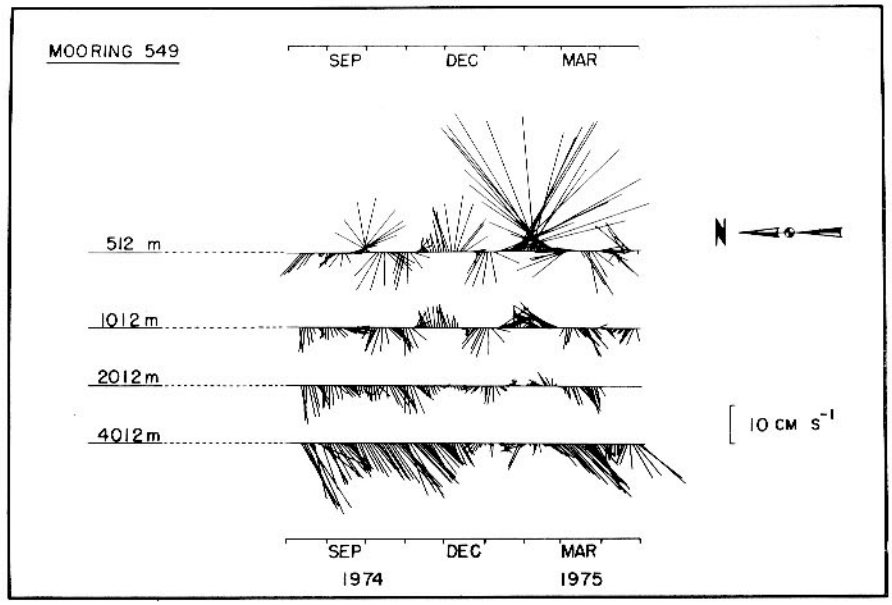
MOORING 549
SEP
DEC
MAR
512 m
1012 m
2012 m
4012 m
N
10 CM S⁻¹
SEP
DEC
MAR
1974
1975

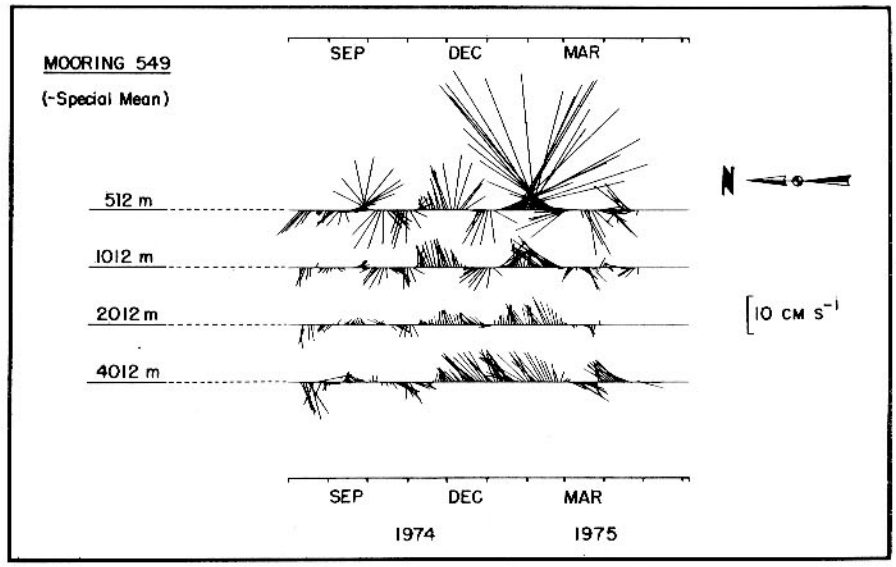
MOORING 549
(-Special Mean)
SEP
DEC
MAR
512 m
1012 m
2012 m
4012 m
N
10 CM S⁻¹
SEP
DEC
MAR
1974
1975

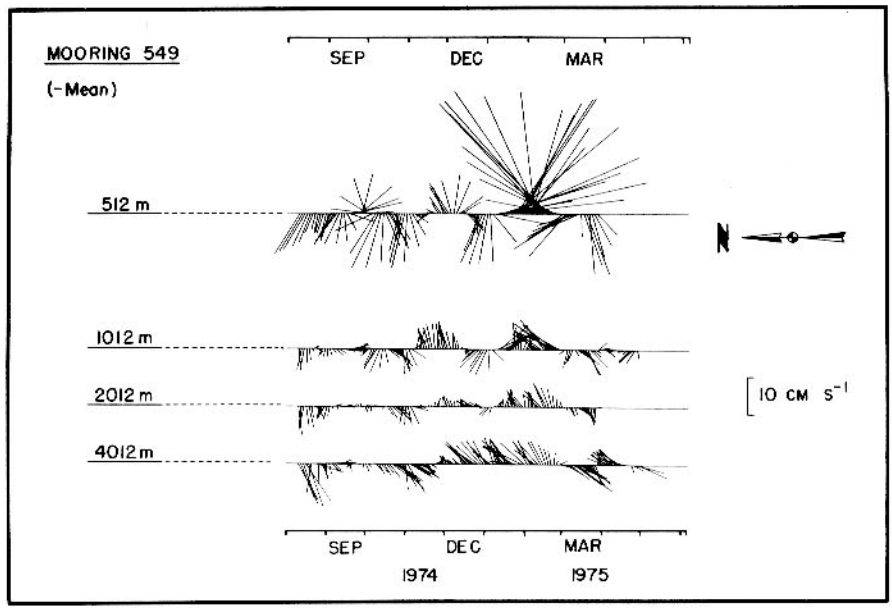
MOORING 549
(-Mean)
SEP
DEC
MAR
512 m
1012 m
2012 m
4012 m
N
10 CM S⁻¹
SEP
DEC
MAR
1974
1975

Fig. 14*c*

TABLE 3. Mean Velocity Components in Centimeters per Second for Mooring 549

Depth, m	$\bar{u}$	$\bar{v}$	$\hat{u}$	$\hat{v}$
512	4.1	−0.8	0.3	−0.4
1012	−1.0	−0.3	−1.6	−0.9
2012	−2.8	−0.9	−4.0	−1.4
4012	−7.0	−4.4	−8.7	−5.7

Variables u and v denote east and north horizontal velocity components, respectively. The overbar denotes record mean, and the circumflex denotes special mean.

trated subtropical gyre [*Worthington*, 1976] with a rather prolific ring population [*Lai and Richardson*, 1977].

Evidence points to the eastern end of the gyre near 40°W as a formation site for eastern rings. J. Gould (personal communication, 1976) detected an eastern ring at the eastern end of the gyre. G. Seaver (personal communication, 1975) detected at least three eastern rings east of 50°W along 34°30'N. Our hydrographic data (Figure 10) show the anomalously high oxygen water in eastern ring cores to have an anomaly intermediate between the normal Sargasso Sea water and the water east of the eastern terminus of the gyre. This is consistent if the eastern rings we observed were not newly formed. If we extrapolate the westward drift of eastern ring A (Figure 5) (4.4 km/d) eastward from 56°30'W in November 1974 to 40°W, it gives about 11 months as an age estimate.

The northern eastern ring along section A-A' in Figure 3 had a 14°C thermostad in its core. This, too, is consistent with an eastern origin. In the southwestern part of the northern gyre of the North Atlantic circulation [*Worthington*, 1976, Figure 42] there is a 14°C thermostad [*Worthington*, 1976, Figure 4] of a nature similar to the 18°C water of the Sargasso gyre [*Worthington*, 1959]. A southwestward meander of the boundary between the gyres would trap water of this type in its core.

Our transport calculation relative to 2000 m (Figure 15) gave an eastern ring cyclonic circulation of about 45×10^6 m³/s. A comparable transport number for the eastern end of the Sargasso gyre can be obtained from *Worthington* [1976] by adding the transports for the water warmer than 4°C. This gives 30 and 59×10^6 m³/s for the two easternmost sections across the gyre boundary. Thus the eastern ring transport is similar to that at the eastern end of the gyre.

Finally, we can summarize what we know or have inferred about the structure of eastern rings: they are cold core current rings of diameter of the order of 200 km, with maximum uplifting of around 450 m (Figure 11). The associated cyclonic transport is about 45×10^6 m³/s (Figures 12 and 15). In their cores the water warmer than about 13°C has a distinct positive oxygen anomaly and a less distinct negative salinity anomaly

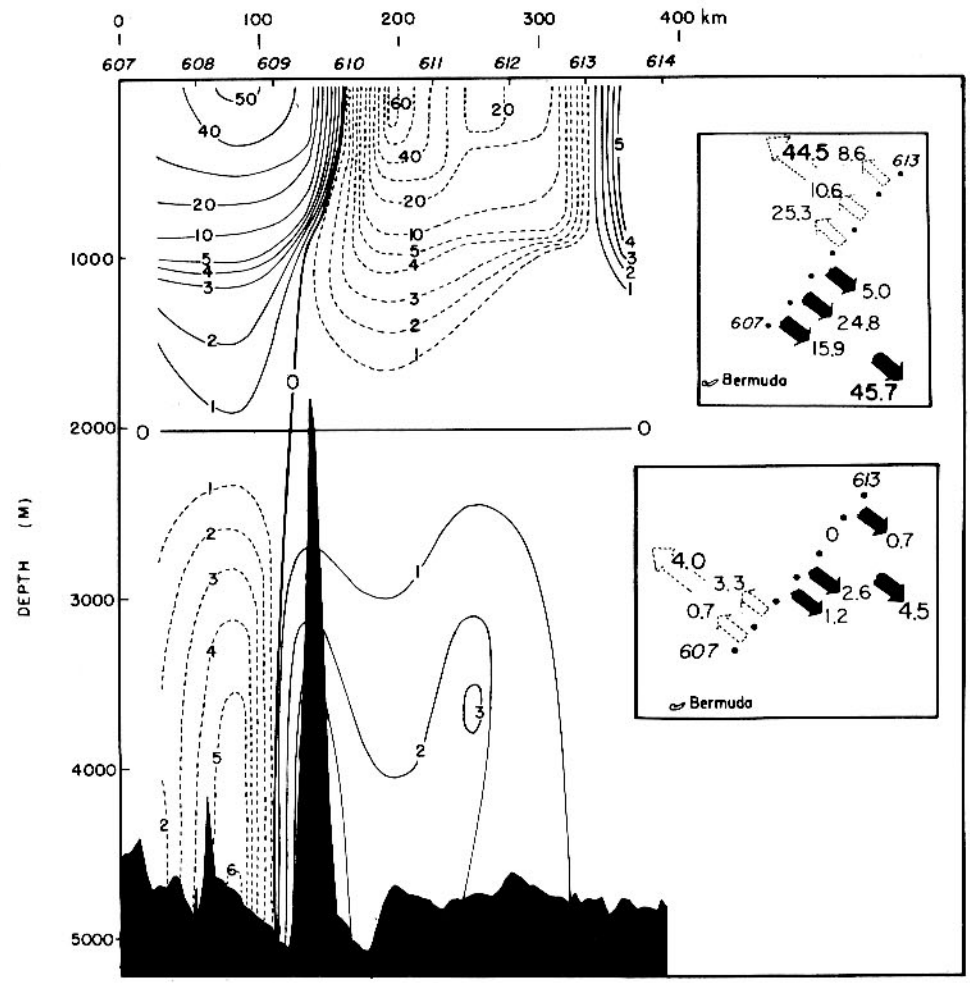

Fig. 15. Geostrophic velocity (in centimeters per second) section and volume transports (in 10^6 m³/s) relative to 2000 m for the deep hydrographic section (Figure 1) across eastern ring A (A_{48} in Figure 9 and Table 2).

(Figure 10). On the basis of current meter data (Figure 13) for one eastern ring they appear to have a level of no motion near 2000 m, with a weak anticyclonic circulation of about 4×10^6 m^3/s below that level (Figure 15). They possibly have a tilted axis, the center lying further south in the deepwater than in the near-surface layers (Figure 11). On several occasions, smaller-scale secondary bumps were seen near eastern rings (Figures 6, 8, and 9 and Table 2), apparently dynamically associated, since the main thermocline did not subside completely in between. Whether these represented collisions with ordinary sized rings or some instability of the eastern ring structure is not known. The eastern rings were old enough when first observed that there was not any obvious direct surface signature such as a warm ring surrounding a cold core. Instead, the effects of eastern rings on the surface water were indirect, affecting the seasonal thermocline gradient during our October-November observations (Figure 4) and causing a distinctly colder mixed layer temperature in our afterwinter observations (Figure 7). The eastern rings appear to drift slightly south of west (Figure 5) at speeds of 2–5 km/d. This path seems to agree with the Sargasso gyre circulation pattern given by *Worthington* [1976].

An obvious question arises, given these observations and our interpretation of them. If eastern rings drift from the east across 60°W, as has been documented clearly for A in Figure 9, then why have they not been detected before? As was mentioned above, things appeared anomalous in the Gulf Stream system during 1974–1975, so it is possible that eastern rings themselves are anomalies and just were not there other years. There are still not enough data available from east of 60°W to determine the representativeness of our observations there. West of 60°W the older mechanical bathythermograph data set is limited by its shallowness. For example, the eastern ring along section F-F' in Figure 6 shows only a colder mixed layer temperature above 200 m to distinguish it from its surroundings. If *Parker*'s [1971] width criterion of 17° at 250 m is used, it is only 72 km wide, the same width he found for the average ring north of 32°N. Clearly, in this case it is only the tip of the iceberg. The mechanical bathythermograph data just are not capable of resolving size well, mainly because 250 m falls in the middle of the 18° water thermostad in the surrounding Sargasso Sea. XBT data can be used for determining size, but this requires different analysis from that performed in the first look by *Lai and Richardson* [1977].

Acknowledgments. This work was supported by the Office of Naval Research under contract N00014-74-C0262, NR083-004, and by the International Decade of Ocean Exploration, Office of the National Science Foundation, under grant OCE 75-03962. Woods Hole Oceanographic Institution contribution 3911. Mid-Ocean Dynamics Experiment (Mode) contribution 93.

References

Barrett, J. R., Available potential energy of Gulf Stream rings, *Deep Sea Res., 18*, 1221–1231, 1971.

Cheney, R. F., and P. L. Richardson, Observed decay of a cyclonic Gulf Stream ring, *Deep Sea Res., 23*, 143–155, 1976.

Dantzler, L., Potential energy maxima in the tropical and subtropical North Atlantic, *J. Phys. Oceanogr., 7*, 512–519, 1977.

Fuglister, F. C., *Atlantic Ocean Atlas, Woods Hole Oceanogr. Inst. Atlas Ser.*, vol. 1, Woods Hole Oceanographic Institution, Woods Hole, Mass., 1960.

Fuglister, F. C., Gulf Stream '60, *Progr. Oceanogr., 1*, 265–373, 1963.

Fuglister, F. C., Cyclonic rings formed by the Gulf Stream, 1965–66, *Stud. Phys. Oceanogr., 1*, 137–167, 1972.

Fuglister, F. C., and L. V. Worthington, Some results of a multiple ship survey of the Gulf Stream, *Tellus, 3*, 1–14, 1951.

Lai, D. Y., and P. L. Richardson, Distribution and movement of Gulf Stream rings, *J. Phys. Oceanogr., 7*, 670–683, 1977.

Parker, C. E., Gulf Stream rings in the Sargasso Sea, *Deep Sea Res., 18*, 981–993, 1971.

Richards, F. A., and A. C. Redfield, Oxygen-density relationships in the western North Atlantic, *Deep Sea Res., 2*, 182–199, 1955.

Schmitz, W. J., On the deep general circulation in the western North Atlantic, *J. Mar. Res., 35*, 21–28, 1977.

Worthington, L. V., The 18° water in the Sargasso Sea, *Deep Sea Res., 5*, 297–305, 1959.

Worthington, L. V., *On the North Atlantic Circulation, Johns Hopkins Oceanogr. Stud.*, vol. 6, The Johns Hopkins University Press, Baltimore, Md., 1976.

(Received January 19, 1977;
revised August 22, 1977;
accepted August 29, 1977.)